ACS OMEGA

http://pubs.acs.org/journal/acsodf

Article

# Electroactive and Stretchable Hydrogels of 3,4-Ethylenedioxythiophene/thiophene Copolymers

Po-Wen Chen, Dian-Huan Ji, You-Sheng Zhang, Celine Lee, and Mei-Yu Yeh*

Cite This: *ACS Omega* 2023, 8, 6753−6761

Read Online

ACCESS | Metrics & More | Article Recommendations | Supporting Information

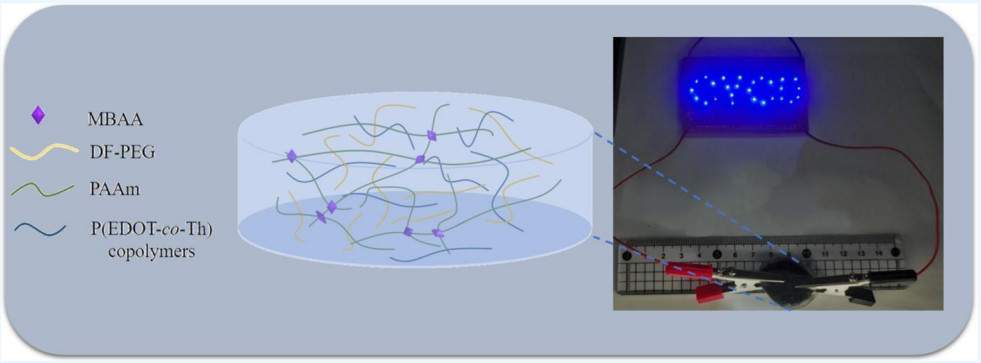


**ABSTRACT:** Hydrogels are conductive and stretchable, allowing for their use in flexible electronic devices, such as electronic skins, sensors, human motion monitoring, brain−computer interface, and so on. Herein, we synthesized the copolymers having various molar ratios of 3,4-ethylenedioxythiophene (EDOT) to thiophene (Th), which served as conductive additives. With doping engineering and incorporation with P(EDOT-*co*-Th) copolymers, hydrogels have presented excellent physical/chemical/electrical properties. It was found that the mechanical strength, adhesion ability, and conductivity of hydrogels were highly dependent on the molar ratio of EDOT to Th of the copolymers. The more the EDOT, the stronger the tensile strength and the greater the conductivity, but the lower the elongation break tends to be. By comprehensively evaluating the physical/chemical/electrical properties and cost of material use, the hydrogel incorporated with a 7:3 molar ratio P(EDOT-*co*-Th) copolymer was an optimal formulation for soft electronic devices.

## INTRODUCTION

Conductive hydrogels are important materials for the fabrication of flexible and wearable electric sensors because of their outstanding designability, good biocompatibility, high stretchability, excellent electrical conductivity, strong adhesion, and so on.[1−10] These well-designed conductive hydrogels have been extensively used in the field of electronic skins,[11−13] wearable devices,[14−16] flexible sensors,[17−19] human motion monitoring,[20,21] and brain−computer interface.[22]

Conductive hydrogels are conductive owing to the incorporation of conductive additives. Conductive additives, for example, carbon nanotubes[23−25] and graphite derivatives,[26,27] were added to the mixture to increase the conductivity of the hydrogels. However, the transmission ability of composite hydrogels remarkably decreased with adding the abovementioned conductive additives.[28] On the contrary, conductive polymers have gained wide attention due to their adjustable mechanical properties, high conductivity, biocompatibility, and ease of preparation.[29−32] Conductive polymers, such as polythiophene (PTh), polyaniline (PANI), polypyrrole (PPy), and poly(*p*-phenylene vinylene) (PPV) have been reported.[33−43] Among these conductive polymers, PTh shows a number of interesting luminescent, electrochromic, electrochemical, and shielding properties, which offer a basis for various new technologies.[44−46] However, the lower electrical stability of PTh during charge/discharge cycles restricted its practical applications.[47] Poly(3,4-ethylenedioxythiophene) (PEDOT) is a kind of thiophene-containing conductive polymer that has excellent electrical, chemical, and environmental stability.[48−50] Recently, several research works had integrated PEDOT with graphene oxide to develop high-performance electronic devices;[51,52] nevertheless, they are relatively more expensive than the conventional conductive polymers, such as PTh. In this work, we aim to obtain cost-effective conductive polymers by fine-tuning the molar ratio of EDOT to Th to development of a novel hydrogel strain sensor.

**Received:** November 16, 2022
**Accepted:** February 2, 2023
**Published:** February 13, 2023

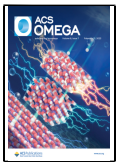





https://doi.org/10.1021/acsomega.2c07368
*ACS Omega* 2023, 8, 6753−6761

Herein, we optimize and develop new conductive hydrogels through adding the different types of P(EDOT-*co*-Th) copolymers (the molar ratios of EDOT/Th were 9:1, 7:3, 5:5, 3:7, and 1:9) to the acrylamide-poly(ethylene glycol)-based hydrogel (control hydrogel). We found that the mechanical, adhesion, and electrical properties of conductive hydrogels were highly dependent on the amount of EDOT of the copolymers. The higher the molar ratio of EDOT to Th, the stronger the tensile strength and the greater conductivity, but the lower the elongation break tends to be. From the Fourier transform infrared spectra, scanning electron microscopy (SEM) images, tensile stress−strain curves, shear strength tests, Nyquist impedance spectra, as well as the cost considerations, the hydrogel incorporated with a 7:3 molar ratio P(EDOT-*co*-Th) copolymer has an optimal mechanical strength, elongation break, adhesion, and electrical performance that might be suitable for electronic skin application.

## RESULTS AND DISCUSSION

**Analysis of P(EDOT-*co*-Th) Copolymers.** In this study, the P(EDOT-*co*-Th) copolymers were synthesized through chemical oxidation polymerization according to the literature procedures.[53,54] The various molar ratios of the EDOT and Th monomers were utilized to prepare a series of P(EDOT-*co*-Th) copolymers (the different feed ratios of EDOT/Th monomers were 9:1, 7:3, 5:5, 3:7, and 1:9, as shown in Table 1). We used

**Table 1. Physical Properties of the P(EDOT-*co*-Th) Copolymers with Different Molar Ratios of Monomers**

| | EDOT/Th | $T_d$ (°C) | particle size (nm) |
|---|---|---|---|
| 1 | 9:1 | 247.8 | 429.3 ± 15.5 |
| 2 | 7:3 | 224.9 | 330.7 ± 10.4 |
| 3 | 5:5 | 224.7 | 319.0 ± 8.7 |
| 4 | 3:7 | 171.2 | 306.3 ± 13.5 |
| 5 | 1:9 | 167.5 | 216.5 ± 19.5 |

Fourier transform infrared spectroscopy (FT-IR), thermogravimetric analysis (TGA), dynamic light scattering (DLS) and contact angle measurement techniques to investigate the properties of P(EDOT-*co*-Th) copolymers. The FT-IR spectra are shown in Figure S1; all of the P(EDOT-*co*-Th) copolymers displayed the absorption bands in the range of 690 to 900 $cm^{-1}$ (C═S stretching vibrations) and 1131 $cm^{-1}$ (C−O−C).[54−57] The absorption bands at 1200, 1332, and 1517 $cm^{-1}$ can be assigned to the stretching of the thiophene moiety.[55−57] In order to understand the decomposition characteristics of the P(EDOT-*co*-Th) copolymers, TGA was used to determine a polymer's thermal stability.[58] As presented in Table 1 and Figure S2, it was observed that when the molar ratio of EDOT increased, higher decomposition temperature was detected. Moreover, DLS was used to analyze the size distribution of P(EDOT-*co*-Th) copolymers in aqueous solution.[57] In Table 1 and Figure S3, we found that the copolymer of P(EDOT-*co*-Th) (9:1) showed the largest particle size with the diameter of 429.3 ± 15.5 nm, probably due to the strong solvation effect between EDOT and water.[53,54] The morphologies of P(EDOT-*co*-Th) copolymers were also measured by SEM, and it was found that the particle sizes were nearly the same as those of their DLS results (Figure S4). We then conducted the contact angle measurement to evaluate hydrophobicity of P(EDOT-*co*-Th) copolymers, the contact angles were all less than 30°, indicating that they could be suitable for applying to artificial electronic skin (Figure S5).

**Preparation of Hydrogels.** After we obtained the P(EDOT-*co*-Th) copolymers, we subsequently prepared a series of conductive hydrogels by adding these copolymers. Furthermore, inspired by click chemistry methods, such as imine, hydrazone, and oxime carbonyl-condensations, we intend to add the dialdehyde-functionalized poly(ethylene glycol) (DF-PEG) to the composition in order to gain good adhesion between the hydrogels and the skin tissue.[59,60] Figure 1 reveals the preparation of conductive hydrogels; the mixtures of acrylamide (AAm), *N*,*N*′-methylenebisacrylamide (MBAA), DF-PEG, P(EDOT-*co*-Th) copolymers, and potassium persulfate (KPS) were stirred and then heated to 70 °C to form stable hydrogels. The optical images of hydrogels are shown in Figure 2. The conductive hydrogels were black (Figure 2b−f); however, the control hydrogel, in the absence of a P(EDOT-*co*-Th) copolymer, was white (Figure 2a). The color differences between conductive and control hydrogels can be

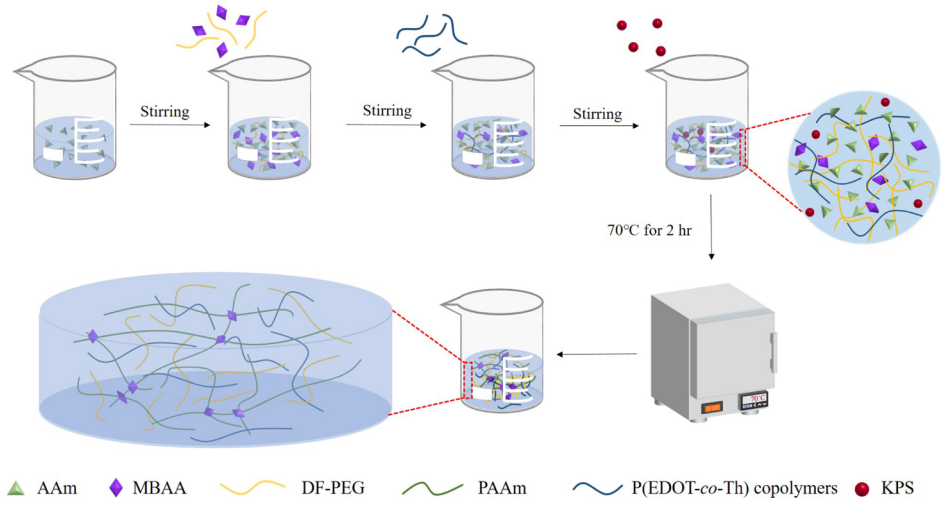


**Figure 1.** Preparation process of conductive hydrogels. [AAm: acrylamide, MBAA: *N*,*N*′-methylenebisacrylamide, DF-PEG: dialdehyde-functionalized poly(ethylene glycol); PAAm: AAm polymers cross-linked by MBAA; P(EDOT-*co*-Th) copolymers, with molar ratios of 9:1, 7:3, 5:5, 3:7, and 1:9; KPS: potassium persulfate].



https://doi.org/10.1021/acsomega.2c07368
ACS Omega 2023, 8, 6753−6761

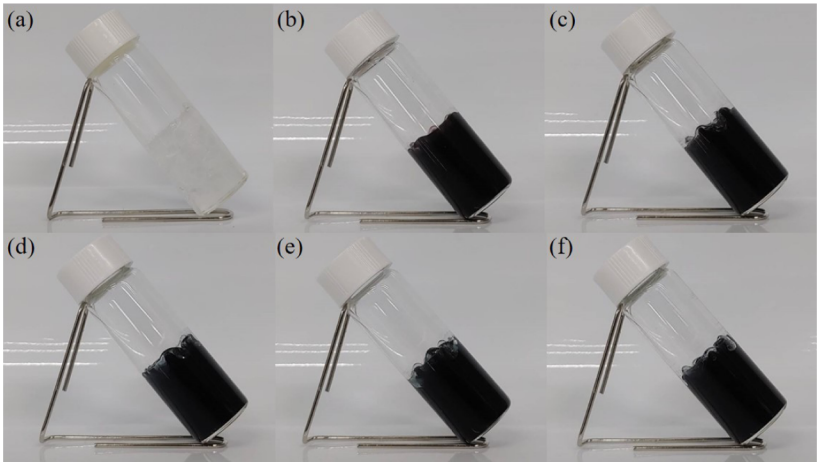


**Figure 2.** Optical images of hydrogels (a) in the absence of P(EDOT-*co*-Th), (b) with P(EDOT-*co*-Th) (9:1), (c) with P(EDOT-*co*-Th) (7:3), (d) with P(EDOT-*co*-Th) (5:5), (e) with P(EDOT-*co*-Th) (3:7), and (f) with P(EDOT-*co*-Th) (1:9).

attributed to the dark blue compound of the P(EDOT-*co*-Th) copolymer.

**Characterization of Hydrogels.** We further investigate the intermolecular interactions of hydrogels incorporated with different kinds of the P(EDOT-*co*-Th) copolymers by the FT-IR method (Figure 3). In the case of the P(EDOT-*co*-Th)

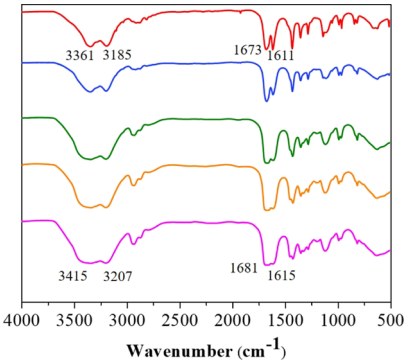


**Figure 3.** FT-IR spectra of hydrogels with P(EDOT-*co*-Th) copolymers, with the molar ratios of 9:1 (red), 7:3 (blue), 5:5 (olive), 3:7 (orange), and 1:9 (magenta).

copolymer, with the molar ratio of 1:9, the absorption frequencies at 3207 and 3415 $cm^{-1}$ can be associated to the N−H stretching vibrations of $NH_2$ group of amide.[61] With increasing the molar ratio of EDOT, for example, the P(EDOT-*co*-Th) copolymer in the molar ratio of 9:1, the $NH_2$ stretching bands appear at the lower frequencies (3185 and 3361 $cm^{-1}$), indicating the formation of hydrogen bonds between molecules.[62,63] Furthermore, the bands assigned to the C═O and C═C modes were also shifted to lower wavenumbers in comparison with the P(EDOT-*co*-Th) copolymer with a molar ratio of 1:9. These observations suggest that the oxygen atoms on EDOT may provide additional intermolecular interactions and thus indicate that the better mechanical performance may be achieved through increasing the molar ratio of EDOT to Th.

**Microstructures of Hydrogels.** Since SEM images offer a variety of morphological and structural information for the characterization of the nanomaterials, it is beneficial to understanding the microstructures of hydrogels incorporated with the P(EDOT-*co*-Th) copolymers.[64,65] As shown in Figure 4a, the nanoparticles with a diameter around 450 nm can be observed in the sample of hydrogel with a 9:1 molar ratio of P(EDOT-*co*-Th) copolymer, which is consistent with the observation of DLS studies (Table1). Meanwhile, SEM images show these particles' tendency to form agglomerates to obtain the continuous and multilayer structures. When reducing the molar ratio of EDOT to Th, the surface connection was decreased, which may be owing to the result of the weaker intermolecular interactions in hydrogel systems.

**Mechanical Properties of Hydrogels.** In order to evaluate the mechanical properties of hydrogels incorporated with different types of the P(EDOT-*co*-Th) copolymers, the stress−strain experiments were carried out using a tensile tester.[66] Figure 5 shows the tensile stress−strain curves of samples, and the measured tensile strengths and elongation breaks were found to be dependent on the composition of the P(EDOT-*co*-Th) copolymers. The tensile strength and elongation break of control hydrogel (in the absence of the P(EDOT-*co*-Th) copolymers) were 32.9 kPa and 60%, respectively. The values of the tensile strengths decreased

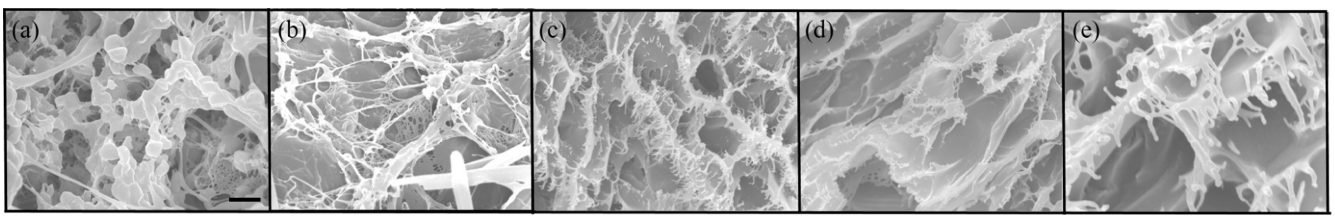


**Figure 4.** SEM images of hydrogels incorporated with the P(EDOT-*co*-Th) copolymers, with the molar ratios of (a) 9:1, (b) 7:3, (c) 5:5, (d) 3:7, and (e) 1:9. Scale bar: 1 $\mu$m.



https://doi.org/10.1021/acsomega.2c07368
*ACS Omega* 2023, 8, 6753−6761

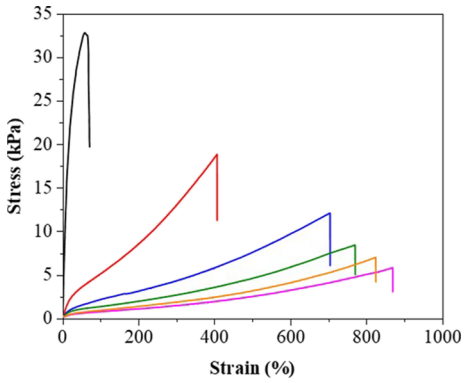


**Figure 5.** Tensile stress−strain curves of hydrogels in the absence of the P(EDOT-*co*-Th) (black) and incorporated with P(EDOT-*co*-Th) copolymers, with the molar ratios of 9:1 (red), 7:3 (blue), 5:5 (olive), 3:7 (orange), and 1:9 (magenta).

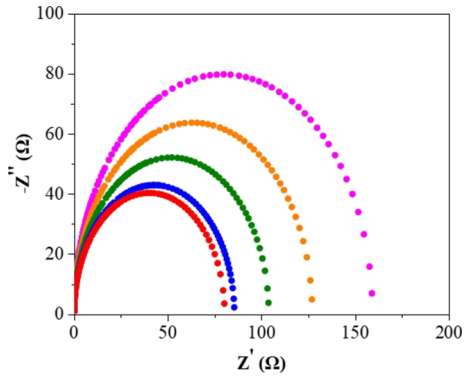


**Figure 6.** Nyquist impedance spectra of hydrogels containing the P(EDOT-*co*-Th) copolymers, with the molar ratios of 9:1 (red), 7:3 (blue), 5:5 (olive), 3:7 (orange), and 1:9 (magenta).

with incorporation of the P(EDOT-*co*-Th) copolymers in hydrogels, but the values of the elongation at break displayed an opposite trend. We then explore the impact of the molar ratio of EDOT to Th in copolymers on mechanical performances; the tensile strengths were 18.7, 12.1, 8.3, 6.9, and 5.6 kPa, in which the molar ratios were 9:1, 7:3, 5:5, 3:7, and 1:9, respectively. The elongation breaks were 406, 705, 771, 824, and 869%, respectively. Moreover, the rheological characterization of hydrogels containing the P(EDOT-*co*-Th) copolymers was performed. As shown in Figure S6, all hydrogels displayed higher storage moduli (G′) than loss moduli (G″) and the dynamic moduli were almost independent of angular frequency (0.1−100 rad/s), confirming the typical gel formation.[67] The G′ values of hydrogels containing the P(EDOT-*co*-Th) copolymers were found to be 5.27, 3.35, 0.39, 0.29, and 0.26 kPa for the molar ratios of 9:1, 7:3, 5:5, 3:7, and 1:9, respectively. It can be concluded from the results of the mechanical experiment of the P(EDOT-*co*-Th) copolymer-containing hydrogels that the higher the molar ratio of EDOT to Th, the stronger the tensile strength and the lower the elongation break tends to be. Swelling tests were carried out to determine the swelling ratio for evaluating the density of the hydrogen bonding network among the hydrogels.[68] The higher the molar ratio of EDOT to Th, the lower was the swelling rate, indicating that the existence of EDOT could increase the crosslink density of hydrogels (Figures S7 and S8). These findings can be supported by FT-IR and SEM studies; the experimental evidences point out that the intermolecular hydrogen bond between oxygen atoms of the EDOT and the amino groups of the AAm units may play an important role in regulating mechanical and swelling behaviors of hydrogels (Figures 3,4 and S8). Additionally, when the shear strength tests of the P(EDOT-*co*-Th) copolymer-containing hydrogels were studied, it was found that the P(EDOT-*co*-Th) copolymers with molar ratios of 9:1 and 7:3 have better adhesion abilities than others (Figure S9). From the abovementioned analysis, it was found that a hydrogel containing a P(EDOT-*co*-Th) copolymer with a 7:3 molar ratio has optimal mechanical strength, elongation break, and adhesion performance.

**Electrical Properties of Hydrogels.** Considering for the flexible electronics applications, the electrical properties of the P(EDOT-*co*-Th) copolymer-containing hydrogels were also measured. Figure 6 presents the impedance spectra of hydrogels; the resistance values of hydrogels containing the P(EDOT-*co*-Th) copolymers with molar ratios of 9:1, 7:3, 5:5, 3:7, and 1:9 were 80, 85, 104, 127, and 159 Ω, respectively. The corresponding calculated conductivities were $3.8 \times 10^3$, $3.6 \times 10^3$, $2.9 \times 10^3$, $2.4 \times 10^3$, and $1.9 \times 10^3$ $\mu$S/cm, indicating that the more amount of EDOT could be helpful for better electrical conductivity.[47−50] Since hydrogels containing 9:1 and 7:3 molar ratio of the P(EDOT-*co*-Th) copolymers exhibited superior electrical properties, the response of stretched gels was investigated using the light-emitting diodes (LEDs). As shown in Figure 7, the LED brightness slightly decreased as the gel was stretched. Notably, a hydrogel containing a copolymer with a 7:3 molar ratio has a larger elongation than that with a molar ratio of 9:1, which is consistent with the observation of the tensile stress−strain experiment (Figure 5). Moreover, the LED lamps displaying the word of CYCU were also confirmed; both gels can light up the LED lamps successfully.

**Substrate's Support and Adhesion.** By comprehensively evaluating the mechanical, adhesion, and electrical properties as well as the cost of material use, the hydrogel incorporated with a 7:3 molar ratio P(EDOT-*co*-Th) copolymer was an optimal formulation to take on for further testing. As can be seen from Figure 8a,b, the strength of hydrogel was good enough to support stainless steel weight under different elongations. Since the hydrogel exhibited good adhesiveness (Figure S5), the adherence of material to different substrates was also studied. As displayed in Figure 8c−f, the hydrogel could adhere to plastic, glass, rubber, and stainless steel weight. Furthermore, the hydrogel has good adhesion before and after bending the finger (Figure 8g,h). The proposed adhesion mechanisms of hydrogels with various substrates are shown in Figure S8. These results demonstrated that the hydrogel incorporated with a 7:3 molar ratio P(EDOT-*co*-Th) copolymer might have the potential to use in the development of artificial electronic skin.

**Conductive Hydrogel Strain Sensor.** To evaluate the potential application of the hydrogel as a strain sensor,[69,70] the hydrogel incorporated with a 7:3 molar ratio P(EDOT-*co*-Th) copolymer was integrated with the finger and it recorded the change in resistance of the strain sensor during finger activities. As illustrated in Figure 9a, the resistance of the sensor responds quickly and repeatedly as the index finger was stretched and bent, suggesting that the fabricated strain sensor exhibits good sensitivity. Furthermore, the index finger was stretched for 1 s and bent for 1, 3, and 5 s, respectively, for five times each, and the performance of the strain sensor was


https://doi.org/10.1021/acsomega.2c07368
ACS Omega 2023, 8, 6753−6761

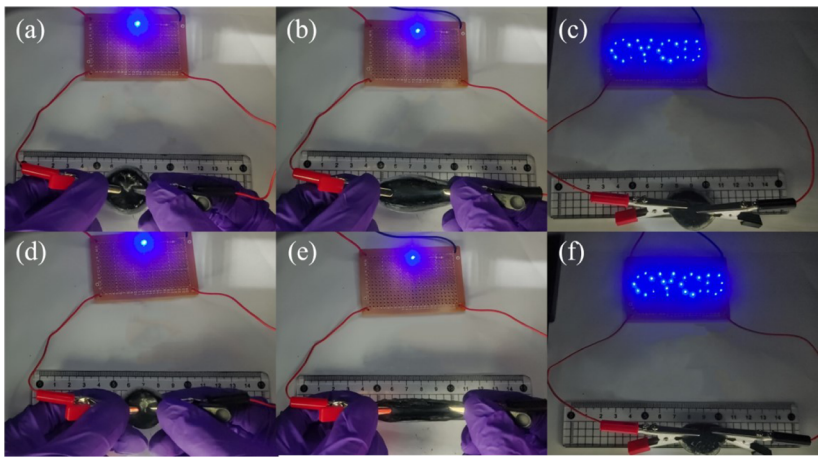


**Figure 7.** (a,b) LED brightness changes under different elongations (0% and ca. 250%) and (c) LED lamps display the word of CYCU of the hydrogel incorporated with a 9:1 molar ratio P(EDOT-*co*-Th) copolymer. (d,e) LED brightness changes under different elongations (0 and 300%) and (f) LED lamps display the word of CYCU of the hydrogel incorporated with a 7:3 molar ratio P(EDOT-*co*-Th) copolymer.

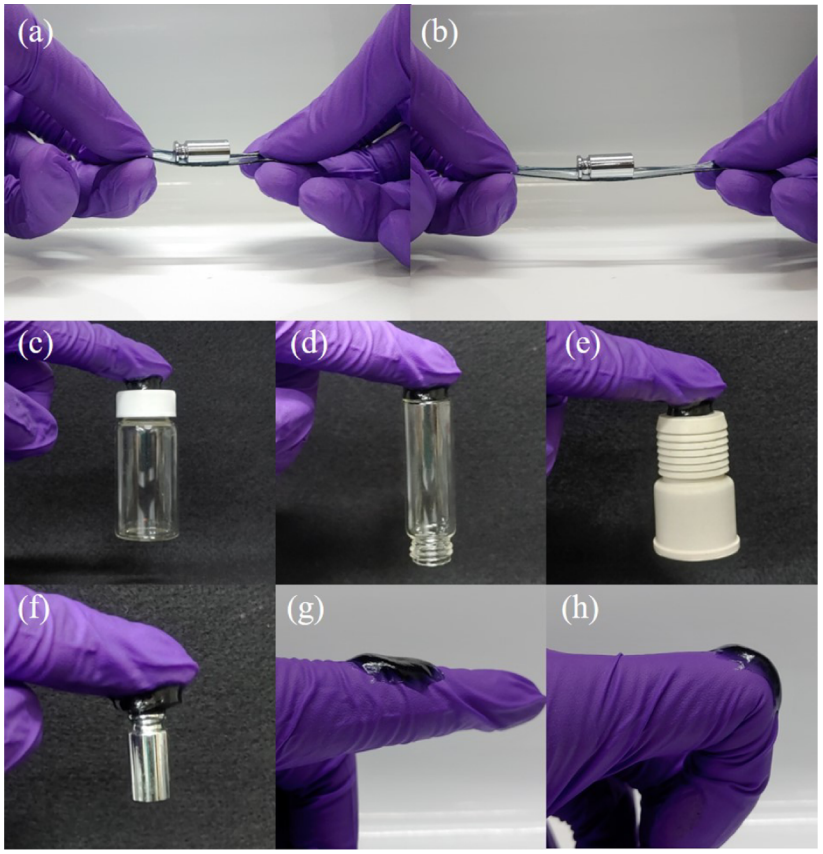


**Figure 8.** Performance of the hydrogel samples (incorporated with a 7:3 molar ratio P(EDOT-*co*-Th) copolymer). (a,b) Support the stainless steel weight under different elongations. Photographs of the hydrogel adhering to different substrates, including (c) plastic, (d) glass, (e) rubber, and (f) stainless steel weight. (g,h) Photographs of hydrogel adherence to the gloves before and after bending the finger.

further evaluated (Figure 9b). Since the hydrogel incorporated with a 7:3 molar ratio P(EDOT-*co*-Th) copolymer has good elongation properties, the hydrogel with different tensile strains (100−500%) was investigated. As can be seen from Figure 9c, the electrical signal could be recorded stably when the hydrogel was at 100, 300, and 500% strain, and during the release process, the electrical signal intensity at the corresponding strain remained almost constant. Then, the cyclic tensile property of the hydrogel was also measured and demonstrated that it exhibits good fatigue resistance characteristics (Figure S10).

## CONCLUSIONS

In this work, a series of P(EDOT-*co*-Th) copolymers have been prepared by varying the molar ratios of EDOT to Th. These copolymers serve as conductive additives and are incorporated into hydrogels to achieve the conductive and stretchable gels. It was found that the mechanical strength,



https://doi.org/10.1021/acsomega.2c07368
*ACS Omega* 2023, 8, 6753−6761

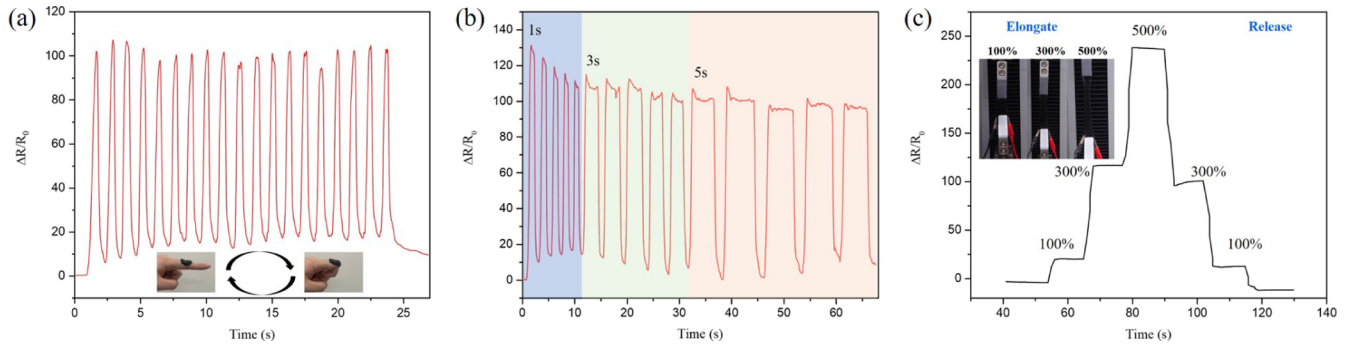


**Figure 9.** Strain sensor of the hydrogel incorporated with a 7:3 molar ratio P(EDOT-*co*-Th) copolymer). (a,b) Relative resistance changes for the stretching and bending of the index finger. (c) Changes in relative resistance under elongation and release.

adhesion ability, and conductivity of hydrogels were highly dependent on the molar ratio of EDOT to Th. The more the EDOT, the stronger the tensile strength and the greater conductivity, but the lower the elongation break tends to be. From the FT-IR spectra, SEM images, tensile stress−strain curves, shear strength tests, Nyquist impedance spectra, and cost of material use, the hydrogel incorporated with a 7:3 molar ratio P(EDOT-*co*-Th) copolymer was an optimal formulation for soft electronic devices.

## EXPERIMENTAL SECTION

**Materials.** Acrylamide (AAm) and MBAA were obtained from Acros Organics. Thiophene and iron (III) chloride anhydrous ($FeCl_3$) were purchased from Alfa Aesar. 4-Formylbenzoic acid, 4-(dimethylamino)pyridine (DMAP), *N*,*N*′-dicyclohexylcarbodiimide (DCC), and KPS were obtained from Sigma-Aldrich. 3,4-Ethylenedioxythiophene (EDOT) was obtained from Tokyo Chemical Industry. Dialdehyde-functionalized poly(ethylene glycol) (DF-PEG) and the P(EDOT-*co*-Th) copolymers were synthesized according to literature procedures.[7,51,52] Briefly, DF-PEG was synthesized by the reaction of 4-formylbenzoic acid (1.33 g, 8.83 mmol), PEG (3.00 g, 1.5 mmol), DMAP (0.11 g, 0.90 mmol), and DCC (1.86 g, 9.00 mmol) at room temperature and precipitated with diethyl ether. P(EDOT-*co*-Th) copolymers, for example, the molar ratio of EDOT/Th = 9:1, was prepared by the reaction mixtures of EDOT (0.95 mL, 9.00 mmol), Th (0.08 mL, 1.00 mmol), and $FeCl_3$ (8.11 g, 50.0 mmol in 12.5 mL of dried $CH_3CN$) in $CH_2Cl_2$ (25 mL) under a nitrogen atmosphere and reaction for 24 h. P(EDOT-*co*-Th) copolymers (EDOT: Th = 7:3, 5:5, 3:7 and 1:9) with different molar ratios were synthesized accordingly.

**Preparation of Hydrogels.** AAm (1.13 g) was dissolved in 2.5 mL of deionized water, and then MBAA (2.50 mg) and DF-PEG (50.00 mg) were added in the reaction mixture. After stirring for 5 min at room temperature, KPS (3.75 mg) was added and the resultant homogeneous solution was heated to 70 °C for 2 h to obtain the control hydrogel. The conductive hydrogels were prepared in a manner similar to that described above, except an additional 5.00 mg of P(EDOT-*co*-Th) copolymers (molar ratio of EDOT/Th were 9:1, 7:3, 5:5, 3:7, and 1:9, respectively) was added to the resultant homogeneous solution to furnish a series of black hydrogels.

**Measurements.** The thermal stabilities and particle sizes of polymers were determined by TGA (DuPont TA Q50) and DLS (Brookhaven 90 Plus-Zeta), respectively. FT-IR (Thermo Fisher Scientific Nicolet iS5) was used to characterize the molecular features and intermolecular forces of the copolymers and hydrogels, respectively. The morphologies of hydrogels were carried out using the SEM (JSM-7600F), and the hydrogel samples were prepared according to our previous report.[8] The rheological measurements of the hydrogels were achieved by a TA rheometer (DHR-1) with a parallel plate setup (diameter of 20 mm and a gap of 1 mm). The mechanical experiments were recorded on a tensile tester (Gotech AI-3000-U). The adhesion strength of the hydrogels was measured by the lap shear test and calculated according to the eq 1

$$\text{lap shear strength (Pa)} = \text{maximum loading force (N)/bonging area (m}^2\text{)} \quad (1)$$

The electrochemical workstation (CHI627E) was used to obtain the electrochemical measurement data of the conductive hydrogels. The sample was fabricated by assembling the conductive hydrogel sheet (the thickness was 0.3 mm) in the middle of two indium tin oxide (ITO) glass substrates. The conductivity ($\sigma$, $\mu$S/cm) was calculated using the eq 2

$$\sigma = L/(R \times A) \quad (2)$$

where $L$, $R$, and $A$ represent the thickness, the resistance, and the cross-sectional area of hydrogels, respectively.

Swelling tests were performed according to the literature method;[68] the equilibrium swelling ratio was calculated using eq 3

$$\text{swelling ratio (\%)} = \frac{W_w - W_0}{W_0} \times 100 \quad (3)$$

where $W_0$ and $W_w$ represent the weight of hydrogels before and after swelling in distilled water, respectively.

## ASSOCIATED CONTENT

### Supporting Information

The Supporting Information is available free of charge at https://pubs.acs.org/doi/10.1021/acsomega.2c07368.

The FT-IR spectra of the P(EDOT-co-Th) copolymers, TGA spectra of the P(EDOT-co-Th) copolymers, summary of the particle sizes of the P(EDOT-co-Th) copolymers, SEM images of the P(EDOT-co-Th) copolymers, contact angles spectra of the P(EDOT-co-Th) copolymers, frequency-dependent rheology measurement of hydrogels incorporated with the P(EDOT-co-Th) copolymers, swelling tests of hydrogels incorporated with the P(EDOT-co-Th) copolymers, proposed intermolecular interactions among the gelators and



https://doi.org/10.1021/acsomega.2c07368
ACS Omega 2023, 8, 6753−6761

adhesion mechanisms of the hydrogels, shear strength tests of hydrogels incorporated with the P(EDOT-co-Th) copolymers, and cyclic tensile property of the hydrogel (PDF)

## AUTHOR INFORMATION


### Corresponding Author

**Mei-Yu Yeh** − *Department of Chemistry, Chung Yuan Christian University, Taoyuan City 320314, Taiwan;* orcid.org/0000-0003-4825-2891; Phone: +886-3-265-3335; Email: myyeh@cycu.edu.tw

### Authors

**Po-Wen Chen** − *Department of Chemistry, Chung Yuan Christian University, Taoyuan City 320314, Taiwan*

**Dian-Huan Ji** − *Department of Chemistry, Chung Yuan Christian University, Taoyuan City 320314, Taiwan*

**You-Sheng Zhang** − *Department of Chemistry, Chung Yuan Christian University, Taoyuan City 320314, Taiwan*

**Celine Lee** − *Department of Chemistry, Chung Yuan Christian University, Taoyuan City 320314, Taiwan*

Complete contact information is available at: https://pubs.acs.org/10.1021/acsomega.2c07368


### Author Contributions

P.-W.C.: Conceptualization, methodology, investigation, data curation, and formal analysis. D.-H.J.: Formal analysis. Y.-S.Z.: Formal analysis. C.L.: Formal analysis. M.-Y.Y.: Supervision, original draft, writing—review and editing, and funding acquisition.

### Notes

The authors declare no competing financial interest.

## ACKNOWLEDGMENTS

This work was supported by the National Science and Technology Council, Taiwan (grant numbers: 110-2113-M-033-006- and 111-2113-M-033-011-)

## ABBREVIATIONS

Th; thiophene; EDOT; 3,4-ethylenedioxythiophene; AAm:; acrylamide; MBAA; *N,N′*-methylene-bisacrylamide; DF-PEG; dialdehyde-functionalized poly(ethylene glycol); KPS; potassium persulfate; FT-IR; Fourier-transform infrared spectroscopy; TGA; thermogravimetric analyzer; DLS; dynamic light scattering; SEM; scanning electron microscopy; LEDs; light-emitting diodes

## REFERENCES


(1) MohanKumar, B. S.; Priyanka, G.; Rajalakshmi, S.; Sankar, R.; Sabreen, T.; Ravindran, J. Hydrogels: potential aid in tissue engineering-a review. *Polym. Bull.* **2022**, *79*, 7009−7039.

(2) Yuk, H.; Lu, B.; Zhao, X. Hydrogel bioelectronics. *Chem. Soc. Rev.* **2019**, *48*, 1642−1667.

(3) Rafieian, S.; Mirzadeh, H.; Mahdavi, H.; Masoumi, M. E. A review on nanocomposite hydrogels and their biomedical applications. *Sci. Eng. Compos. Mater.* **2019**, *26*, 154−174.

(4) Lee, K. Y.; Mooney, D. J. Hydrogels for Tissue Engineering. *Chem. Rev.* **2001**, *101*, 1869−1880.

(5) Gu, Y.; Zhang, T.; Chen, H.; Wang, F.; Pu, Y.; Gao, C.; Li, S. Mini Review on Flexible and Wearable Electronics for Monitoring Human Health Information. *Nanoscale Res. Lett.* **2019**, *14*, 263.

(6) Bao, Z.; Chen, X. Flexible and Stretchable Devices. *Adv. Mater.* **2016**, *28*, 4177−4179.

(7) Wang, H.-J.; Chu, Y.-Z.; Chen, C.-K.; Liao, Y.-S.; Yeh, M.-Y. Preparation of conductive self-healing hydrogels via an interpenetrating polymer network method. *RSC Adv.* **2021**, *11*, 6620−6627.

(8) Chen, C.-K.; Chen, P.-W.; Wang, H.-J.; Yeh, M.-Y. Alkyl Chain Length Effects of Imidazolium Ionic Liquids on Electrical and Mechanical Performances of Polyacrylamide/Alginate-Based Hydrogels. *Gels* **2021**, *7*, 164.

(9) Wang, Z.; Cong, Y.; Fu, J. Stretchable and tough conductive hydrogels for flexible pressure and strain sensors. *J. Mater. Chem. B* **2020**, *8*, 3437−3459.

(10) Park, J.; Jeon, N.; Lee, S.; Choe, G.; Lee, E.; Lee, J. Y. Conductive hydrogel constructs with three-dimensionally connected graphene networks for biomedical applications. *Chem. Eng. J.* **2022**, *446*, 137344.

(11) Li, C. Towards conductive hydrogels in e-skins: a review on rational design and recent developments. *RSC Adv* **2021**, *11*, 33835−33848.

(12) Cheng, X.; Zhang, F.; Dong, W. Soft Conductive Hydrogel-Based Electronic Skin for Robot Finger Grasping Manipulation. *Polymers* **2022**, *14*, 3930.

(13) Zhang, Z.; Chen, Z.; Wang, Y.; Zhao, Y. Bioinspired conductive cellulose liquid-crystal hydrogels as multifunctional electrical skins. *Proc. Natl. Acad. Sci. U.S.A.* **2020**, *117*, 18310−18316.

(14) Chen, Z.; Chen, Y.; Hedenqvist, M. S.; Chen, C.; Cai, C.; Li, H.; Liu, H.; Fu, J. Multifunctional conductive hydrogels and their applications as smart wearable devices. *J. Mater. Chem. B* **2021**, *9*, 2561−2583.

(15) Zhang, L.; Wang, J.; Wang, S.; Wang, L.; Wu, M. Neuron-inspired multifunctional conductive hydrogels for flexible wearable sensors. *J. Mater. Chem. C* **2022**, *10*, 4327−4335.

(16) Wang, X.; Bai, Z.; Zheng, M.; Yue, O.; Hou, M.; Cui, B.; Su, R.; Wei, C.; Liu, X. Engineered gelatin-based conductive hydrogels for flexible wearable electronic devices: Fundamentals and recent advances. *J. Sci.: Adv. Mater. Devices* **2022**, *7*, 100451.

(17) Zhang, H.; Yue, M.; Wang, T.; Wang, J.; Wu, X.; Yang, S. Conductive hydrogel-based flexible strain sensors with superior chemical stability and stretchability for mechanical sensing in corrosive solvents. *New J. Chem.* **2021**, *45*, 4647−4657.

(18) Wang, F.; Li, Z.; Guo, J.; Liu, L.; Fu, H.; Yao, J.; Krucińska, I.; Draczyński, Z. Highly Strong, Tough, and Stretchable Conductive Hydrogels Based on Silk Sericin-Mediated Multiple Physical Interactions for Flexible Sensors. *ACS Appl. Polym. Mater.* **2022**, *4*, 618−626.

(19) Li, G.; Li, C.; Li, G.; Yu, D.; Song, Z.; Wang, H.; Liu, X.; Liu, H.; Liu, W. Development of Conductive Hydrogels for Fabricating Flexible Strain Sensors. *Small* **2021**, *18*, 2101518.

(20) Ren, J.; Li, M.; Li, R.; Wang, X.; Li, Y.; Yang, W. Transparent, highly stretchable, adhesive, and sensitive ionic conductive hydrogel strain sensor for human motion monitoring. *Colloids Surf. A* **2022**, *652*, 129795.

(21) Chen, L.; Chang, X.; Chen, J.; Zhu, Y. Ultrastretchable, Antifreezing, and High-Performance Strain Sensor Based on a Muscle-Inspired Anisotropic Conductive Hydrogel for Human Motion Monitoring and Wireless Transmission. *ACS Appl. Mater. Interfaces* **2022**, *14*, 43833−43843.

(22) Wang, X.; Sun, X.; Gan, D.; Soubrier, M.; Chiang, H.-Y.; Yan, L.; Li, Y.; Li, J.; Yu, S.; Xia, Y.; Wang, K.; Qin, Q.; Jiang, X.; Han, L.; Pan, T.; Xie, C.; Lu, X. Bioadhesive and conductive hydrogel-integrated brain-machine interfaces for conformal and immune-evasive contact with brain tissue. *Matter* **2022**, *5*, 1204−1223.

(23) Hsiao, L.-Y.; Jing, L.; Li, K.; Yang, H.; Li, Y.; Chen, P.-Y. Carbon nanotube-integrated conductive hydrogels as multifunctional robotic skin. *Carbon* **2020**, *161*, 784−793.

(24) Ye, L.; Ji, H.; Liu, J.; Tu, C.-H.; Kappl, M.; Koynov, K.; Vogt, J.; Butt, H.-J. Carbon Nanotube-Hydrogel Composites Facilitate Neuronal Differentiation While Maintaining Homeostasis of Network Activity. *Adv. Mater.* **2021**, *33*, 2102981.

(25) He, J.; Shi, M.; Liang, Y.; Guo, B. Conductive adhesive self-healing nanocomposite hydrogel wound dressing for photothermal therapy of infected full-thickness skin wounds. *Chem. Eng. J.* **2020**, *394*, 124888.
(26) Chuah, S.; Pan, Z.; Sanjayan, J. G.; Wang, C. M.; Duan, W. H. Nano reinforced cement and concrete composites and new perspective from graphene oxide. *Constr. Build. Mater.* **2014**, *73*, 113−124.
(27) Lee, C.; Wei, X.; Kysar, J. W.; Hone, J. Measurement of the Elastic Properties and Intrinsic Strength of Monolayer Graphene. *Science* **2008**, *321*, 385−388.
(28) Liu, K.; Wei, S.; Song, L.; Liu, H.; Wang, T. Conductive Hydrogels-A Novel Material: Recent Advances and Future Perspectives. *J. Agric. Food Chem.* **2020**, *68*, 7269−7280.
(29) K, N.; Rout, C. S. Conducting polymers: a comprehensive review on recent advances in synthesis, properties and applications. *RSC Adv.* **2021**, *11*, 5659−5697.
(30) Pavel, I.-A.; Lakard, S.; Lakard, B. Flexible Sensors Based on Conductive Polymers. *Chemosensors* **2022**, *10*, 97.
(31) Chapman, C. A. R.; Cuttaz, E. A.; Goding, J. A.; Green, R. A. Actively Controlled Local Drug Delivery Using Conductive Polymer-Based Devices. *Appl. Phys. Lett.* **2020**, *116*, 010501.
(32) Nezakati, T.; Seifalian, A.; Tan, A.; Seifalian, A. M. Conductive Polymers: Opportunities and Challenges in Biomedical Applications. *Chem. Rev.* **2018**, *118*, 6766−6843.
(33) Kaloni, T. P.; Giesbrecht, P. K.; Schreckenbach, G.; Freund, M. S. Polythiophene: From Fundamental Perspectives to Applications. *Chem. Mater.* **2017**, *29*, 10248−10283.
(34) McCullough, R. D. The Chemistry of Conducting Polythiophenes. *Adv. Mater.* **1998**, *10*, 93−116.
(35) Yan, B.; Chen, Z.; Cai, L.; Chen, Z.; Fu, J.; Xu, Q. Fabrication of polyaniline hydrogel: Synthesis, characterization and adsorption of methylene blue. *Appl. Surf. Sci.* **2015**, *356*, 39−47.
(36) Brahim, S.; Narinesingh, D.; Guiseppi-Elie, A. Polypyrrole-hydrogel composites for the construction of clinically important biosensors. *Biosens. Bioelectron.* **2002**, *17*, 53−59.
(37) Wu, Y.; Chen, Y. X.; Yan, J.; Yang, S.; Dong, P.; Soman, P. Fabrication of conductive polyaniline hydrogel using porogen leaching and projection microstereolithography. *J. Mater. Chem. B* **2015**, *3*, 5352−5360.
(38) Gong, H. Y.; Park, J.; Kim, W.; Kim, J.; Lee, J. Y.; Koh, W.-G. A Novel Conductive and Micropatterned PEG-Based Hydrogel Enabling the Topographical and Electrical Stimulation of Myoblasts. *ACS Appl. Mater. Interfaces* **2019**, *11*, 47695−47706.
(39) Orduño Rodríguez, A. M.; Pérez Martínez, C. J.; del Castillo Castro, T.; Castillo Ortega, M. M.; Rodríguez Félix, D. E.; Romero García, J. Nanocomposite hydrogel of poly(vinyl alcohol) and biocatalytically synthesized polypyrrole as potential system for controlled release of metoprolol. *Polym. Bull.* **2020**, *77*, 1217−1232.
(40) Yang, C.; Yin, J.; Chen, Z.; Du, H.; Tian, M.; Zhang, M.; Zheng, J.; Ding, L.; Zhang, P.; Zhang, X.; et al. Highly Conductive, Stretchable, Adhesive, and Self-Healing Polymer Hydrogels for Strain and Pressure Sensor. *Macromol. Mater. Eng.* **2020**, *305*, 2000479.
(41) Eftekhari, B. S.; Eskandari, M.; Janmey, P. A.; Samadikuchaksaraei, A.; Gholipourmalekabadi, M. Conductive chitosan/polyaniline hydrogel with cell-imprinted topography as a potential substrate for neural priming of adipose derived stem cells. *RSC Adv.* **2021**, *11*, 15795−15807.
(42) Duan, J.; Liang, X.; Guo, J.; Zhu, K.; Zhang, L. Ultra-Stretchable and Force-Sensitive Hydrogels Reinforced with Chitosan Microspheres Embedded in Polymer Networks. *Adv. Mater.* **2016**, *28*, 8037−8044.
(43) Kaur, G.; Adhikari, R.; Cass, P.; Bown, M.; Gunatillake, P. Electrically conductive polymers and composites for biomedical applications. *RSC Adv.* **2015**, *5*, 37553−37567.
(44) Englebienne, P.; Weiland, M. Synthesis of water-soluble carboxylic and acetic acid-substituted poly(thiophenes) and the application of their photochemical properties in homogeneous competitive immunoassays. *Chem. Commun.* **1996**, 1651−1652.
(45) Fujitsuka, M.; Sato, T.; Segawa, H.; Shimidzu, T. Photochemical polymerization of oligothiophene and dithienothiophene. *Synth. Met.* **1995**, *69*, 309−310.
(46) Li, G.; Koßmehl, G.; Welzel, H.-P.; Engelmann, G.; Hunnius, W.-D.; Plieth, W.; Zhu, H. Reactive groups on polymer coated electrodes, 7. New electrogenerated electroactive polythiophenes with different protected carboxyl groups. *Macromol. Chem. Phys.* **1998**, *199*, 525−533.
(47) Min, J. H.; Patel, M.; Koh, W.-G. Incorporation of Conductive Materials into Hydrogels for Tissue Engineering Applications. *Polymers* **2018**, *10*, 1078.
(48) Ajmal Mokhtar, S. M.; Alvarez de Eulate, E.; Sethumadhavan, V.; Yamada, M.; Prow, T. W.; Evans, D. R. Electrochemical stability of PEDOT for wearable on-skin application. *J. Appl. Polym. Sci.* **2021**, *138*, 51314.
(49) Zhou, S.; Xia, D.; Liang, S.; Liu, B.; Wang, J.; Xiao, C.; Tang, Z.; Li, W. Enhancing the Performance of Small-Molecule Organic Solar Cells via Fused-Ring Design. *ACS Appl. Mater. Interfaces* **2022**, *14*, 7093−7101.
(50) Mawad, D.; Artzy-Schnirman, A.; Tonkin, J.; Ramos, J.; Inal, S.; Mahat, M. M.; Darwish, N.; Zwi-Dantsis, L.; Malliaras, G. G.; Gooding, J. J.; et al. Electroconductive Hydrogel Based on Functional Poly(Ethylenedioxy Thiophene). *Chem. Mater.* **2016**, *28*, 6080−6088.
(51) Gan, D.; Huang, Z.; Wang, X.; Jiang, L.; Wang, C.; Zhu, M.; Ren, F.; Fang, L.; Wang, K.; Xie, C.; Lu, X. Graphene Oxide-Templated Conductive and Redox-Active Nanosheets Incorporated Hydrogels for Adhesive Bioelectronics. *Adv. Funct. Mater.* **2020**, *30*, 1907678.
(52) Liu, F.; Xie, L.; Wang, L.; Chen, W.; Wei, W.; Chen, X.; Luo, S.; Dong, L.; Dai, Q.; Huang, Y.; Wang, L. Hierarchical Porous RGO/PEDOT/PANI Hybrid for Planar/Linear Supercapacitor with Outstanding Flexibility and Stability. *Nano-Micro Lett.* **2020**, *12*, 17.
(53) Gursoy, S.; Yildiz, A.; Cogal, G. C.; Gursoy, O. A novel lactose biosensor based on electrochemically synthesized 3,4-ethylenedioxythiophene/thiophene (EDOT/Th) copolymer. *Open Chem.* **2020**, *18*, 974−985.
(54) Massoumi, B.; Alipour, N.; Fathalipour, S.; Jaymand, M. Nanostructured poly(2,2′-bithiophene-co-3,4-ethylenedioxythiophene). *High Perform. Polym.* **2015**, *27*, 161−170.
(55) Lee, S.; Gleason, K. K. Enhanced Optical Property with Tunable Band Gap of Cross-linked PEDOT Copolymers via Oxidative Chemical Vapor Deposition. *Adv. Funct. Mater.* **2015**, *25*, 85−93.
(56) M, P. R.; Berchmans, S. Poly (3, 4-ethylene dioxythiophene) Supported Palladium Catalyst prepared by Galvanic Replacement Reaction for Methanol Tolerant Oxygen Reduction. *Sci. Rep.* **2019**, *9*, 19184.
(57) Ryu, H. W.; Kim, Y. S.; Kim, J. H.; Cheong, I. W. Direct synthetic route for water-dispersible polythiophene nanoparticles via surfactant-free oxidative polymerization. *Polymer* **2014**, *55*, 806−812.
(58) Abdolmaleki, A.; Mohamadi, Z.; Rezaei, B.; Askarpour, N. Synthesis of small-band gap poly(3,4-ethylenedioxythiophene methine)s using acidic ionic liquids as catalyst. *Polym. Bull.* **2013**, *70*, 665−679.
(59) Collins, J.; Xiao, Z.; Müllner, M.; Connal, L. A. The Emergence of Oxime Click Chemistry and its Utility in Polymer Science. *Polym. Chem.* **2016**, *7*, 3812−3826.
(60) Grover, G. N.; Lam, J.; Nguyen, T. H.; Segura, T.; Maynard, H. D. Biocompatible Hydrogels by Oxime Click Chemistry. *Biomacromolecules* **2012**, *13*, 3013−3017.
(61) Zheng, Y.; Liang, Y.; Zhang, D.; Sun, X.; Liang, L.; Li, J.; Liu, Y.-N. Gelatin-Based Hydrogels Blended with Gellan as an Injectable Wound Dressing. *ACS Omega* **2018**, *3*, 4766−4775.
(62) Schäfer, S.; Kickelbick, G. Double Reversible Networks: Improvement of Self-Healing in Hybrid Materials via Combination of Diels-Alder Cross-Linking and Hydrogen Bonds. *Macromolecules* **2018**, *51*, 6099−6110.
(63) Rao, C. N. R.; Chaturvedi, G. C.; Gosavi, R. K. Infrared spectra and configurations of alkylurea derivatives: Normal vibrations on N,


https://doi.org/10.1021/acsomega.2c07368
*ACS Omega* 2023, 8, 6753−6761

N′-dimethyl- and tetramethylurea. *J. Mol. Spectrosc.* **1968**, *28*, 526−535.
(64) Dolgov, L.; Yaroshchuk, O.; Qiu, L. SEM investigations of the polymer morphology in the liquid crystal-polymer composites with different polymer contents. *Mol. Cryst. Liq. Cryst.* **2007**, *468*, 335−344.
(65) Daniel, S.; Thomas, S. Scanning Electron Microscopy as a Powerful Morphological Characterization Technique for Polymer Blends and Polymer Nanocomposites. in *Microscopy Applied to Materials Sciences and Life Sciences*, 1st ed.; Rane, A.V.; Thomas, S.; Kalarikkal, N., Ed.; Academic Press: New Jersey, 2018; pp 3-34.
(66) Wang, J.; Lin, Y.; Mohamed, A.; Ji, Q.; Jia, H. High strength and flexible aramid nanofiber conductive hydrogels for wearable strain sensors. *J. Mater. Chem. C* **2021**, *9*, 575−583.
(67) Raveendran, R. L.; Devaki, S. J. Design and Development of Biogel Through Hierarchical Self-Organisation of Biomolecule for Sustainable Antibacterial Applications. *ChemistrySelect* **2018**, *3*, 3825−3831.
(68) Cao, L.; Zhao, Z.; Wang, X.; Huang, X.; Li, J.; Wei, Y. Tough, Antifreezing, and Conductive Hydrogel Based on Gelatin and Oxidized Dextran. *Adv. Mater. Technol.* **2022**, *7*, 2101382.
(69) Deng, Z.; Hu, T.; Lei, Q.; He, J.; Ma, P. X.; Guo, B. Stimuli-Responsive Conductive Nanocomposite Hydrogels with High Stretchability, Self-Healing, Adhesiveness, and 3D Printability for Human Motion Sensing. *ACS Appl. Mater. Interfaces* **2019**, *11*, 6796−6808.
(70) Deng, Z.; Guo, Y.; Zhao, X.; Ma, P. X.; Guo, B. Multifunctional Stimuli-Responsive Hydrogels with Self-Healing, High Conductivity, and Rapid Recovery through Host-Guest Interactions. *Chem. Mater.* **2018**, *30*, 1729−1742.


https://doi.org/10.1021/acsomega.2c07368
*ACS Omega* 2023, 8, 6753−6761